

MINERALOGICAL CHARACTERIZATION AND SORPTION PROPERTIES OF GOETHITE RICH IRON ORE FROM DAITARI, ORISSA, INDIA

R.K. Behera, K. Rout, B. Nayak¹ and N.N. Das

Department of Chemistry, North Orissa University, Baripada, Orissa - 757003, India

¹MNP Division, National Metallurgical Laboratory, Jamshedpur - 831007, India

ABSTRACT

The present study was an attempt to find alternative uses of goethite rich iron ore, usually not used as raw material for iron extraction, as an adsorbent for removal of anionic contaminants from water. Mineralogical characterization by optical microscope, XRD revealed the presence of substantial amount goethite in the iron ore which was also supported from the TG-DTA and FT-IR results. On heating in air, the goethite content was completely converted to hematite at 400°C. The sorption behaviour of the untreated (GRI-0) and heat treated iron ore were studied using aqueous phosphate solution as the adsorbate with respect to effect of pH, initial phosphate concentration, amount of adsorbent, interfering anions and heat treatment. Phosphate uptake was seen to increase with increasing temperature of heat treatment, attains a maximum value at 300°C and thereafter decreased on further increase of temperature. The experimental equilibrium adsorption data were fitted well to Langmuir isotherm model. The complete desorption of adsorbed phosphate at pH \geq 12.0 indicated the adsorption of phosphate was reversible and may be reused further. The results obtained could be useful for considering GRI-0 as adsorbent for removal of phosphate ions from contaminated water bodies.

Keywords: *Goethite, Iron ores, Mineralogical characterization, Sorption, Phosphate.*

INTRODUCTION

Iron bearing ores are among several naturally occurring minerals that have been exploited for alternative applications apart from their large scale use as raw materials for iron extraction. The presence of structural water, primarily in the form of oxyhydroxides, in these ores cause serious problems in blast furnace operations which limit their direct use for iron extraction. Often a pre-treatment like sintering of these iron ores is required prior to their use in iron extraction. On the other hand, iron ores with substantial amount iron in the form of oxyhydroxides is beneficial to enhance the adsorbing and catalytic properties of the minerals. The use of synthetic iron hydr(oxides) as adsorbents for several water polluting anionic and cationic species like SeO_3^{2-} / SeO_4^{2-} , AsO_3^{2-} / AsO_4^{2-} , HPO_4^{2-} / PO_4^{3-} , F^- , Pb^{2+} , Cd^{2+} , Hg^{2+} etc. as well dyes has been extensively studied.^[1-5] However, compared to these synthetic minerals, the naturally occurring iron hydr(oxides) such as hematite, ferrihydrite, goethite and lepidocrocite are often found more attractive adsorbents because of their low cost and availability in different particle sizes. As a result several studies have been made during last decade to use iron bearing minerals as adsorbents

for removal of polluting species from wastewaters.^[5-11] The catalytic activity is another important property of iron bearing minerals that has been exploited extensively in recent years. Both synthetic and naturally occurring iron hydr (oxides) have used as catalysts/photocatalysts in oxidation of a variety of organic water pollutants like phenols, dye etc.^[12-16]

Keeping the above in view, the primary objectives of the present study are to (i) characterize the proposed natural materials with respect to their chemical and mineralogical compositions, and (ii) investigate the potential of selected mineral as an adsorbent for removal anionic pollutants from wastewater with special reference to phosphate which is responsible for eutrophication and affects many natural water bodies.^[16]

EXPERIMENTAL

Materials

Iron ore samples were collected from Daitari, Keonjhar open cast mines of Orissa Mining Corporation Ltd. as iron ore fines. These fines, size range in between -0.5 mm to $+10$ mm, were grinded to 100 mesh size for further use. Based on the chemical analyses, a typical sample with following composition (Table 1) was selected for further studies. Preliminary studies revealed that the iron ore contains a sizeable amount of water and goethite as a major phase. Thus it would be interesting to see the effect of thermal treatment on the mineral phases of iron ore and also on adsorption properties. For this a weighed amount of untreated iron ore (GRI-0) was thermally treated in air at 100, 200, 300, 400 and 500°C for 3 h and represented as GRI-100, GRI-200, GRI-300, GRI-400 and GRI-500, respectively. The weight losses after thermal treatment were determined and used to estimate the loss of water and other volatiles, if any.

Methods

Chemical analyses of the ores were carried by conventional wet chemical and also by XRF (Phillips, Axios 4 kW). Powder XRD of representative samples, both untreated and heat treated, were carried out by a X-ray Diffractometer (Phillips, PW3710) using CuK_α radiation at a scan speed of 2°min^{-1} . Optical micrographs were taken using an optical microscope. TG-DTA of untreated sample was carried out in air using a Shimadzu DT 40 Thermal analyzer (SDT Q 60) in the temperature range 30–1000°C at a heating rate of $10^\circ\text{C}/\text{min}$. FT-IR spectra of different samples in KBr phase were recorded using a ThermoNicolet 870 FT-IR averaging 32 scans and at a resolution of 4 cm^{-1} . The points of zero charge (pH_{zpc} 's) were determined by batch acid-base titration technique.^[17]

The efficiency of fresh and heat treated goethite rich iron ore as adsorbents was assessed for phosphate adsorption by batch equilibrium method under varying experimental parameters like pH, adsorption time, adsorbent amount, phosphate concentration, presence interfering ions etc. In a typical experiment, 50 mL of aqueous dihydrogen phosphate solution of desired concentration was mixed with an appropriate amount of adsorbent (GRIs) in a 100 mL stoppered conical flasks. The initial phosphate concentration and amount of adsorbent were varied from 5–50 mg P L^{-1} and 2.0–10.0 g L^{-1} , respectively. The solutions were adjusted to desired pH by addition of dilute NaOH or HCl; the volume of NaOH or HCl was never exceeding 0.5 ml. The flasks were shaken in a water shaker bath at $30.0 \pm 0.1^\circ\text{C}$ with a constant stroke (100 rpm) until the solution was attained the equilibrium (~ 6 h). The samples, taken at regular intervals, were centrifuged and phosphate concentrations were determined spectrophotometrically by standard phosphovanado-

molybdate method. The amount of phosphate adsorbed was determined from the ratio of phosphate in the solution and particulate phases using the following equation,

$$q_e = (C_i - C_e)V/m \quad \dots (1)$$

Where q_e , C_i , C_e , V and m represent the amount of P adsorbed on the solid (mgP g^{-1}), the initial concentration (mg L^{-1}), the final concentration (mg L^{-1}), volume of the solution (L) and amount of adsorbent (g), respectively.

The desorption/regeneration experiments were carried out by treating the 0.1 g adsorbent, loaded with phosphate under optimized set of conditions ($\text{pH} \sim 5.0$, 10 mgP L^{-1}), with 40 ml distilled water adjusted to different pH in the range 4.0 to 12.0 using aqueous solution of NaOH and then mechanically stirred for 2 h at room temperature. The desorbed phosphate in the solution was determined spectrophotometrically. The regenerated GRI was washed with distilled water in the centrifuge tube and transferred to the 100 ml conical flask for treatment with fresh phosphate solution (10 mgP L^{-1}) at $\text{pH} \sim 5.0$. The amount of phosphate adsorbed by the regenerated GRI was determined after shaking for 6 h.

RESULTS AND DISCUSSION

Physicochemical characterization

The chemical analyses of representative sample (GRI-0) show Fe as the main constituent while Al and Si as the minor constituents (Table 1). The other constituents contribute less than 0.5 %. It is seen that the sample contains substantial amount of water. The optical micrograph (Fig. 1a) shows that the untreated iron ore contains dominantly goethite (dark grey) along with minor amounts of hematite (whitish). The black portions are due to cavities partially filled with clayey matter. On heating at 400°C , goethite phase is completely converted to hematite due to loss of structural water (Fig. 1b). This is evident from the change in colour from dark-grey to whitish along with increase of reflectivity as well as disappearance of original grain-boundary between goethite and hematite. The PXRD patterns of untreated sample also exhibit (Fig. 2) the characteristic peaks of goethite in the untreated ores due to presence of substantial amount goethite. The other iron phases in the untreated ore are hematite and magnetite. On heating, the goethite phase is progressively converted to hematite and the characteristics goethite peaks are completely disappeared at 400°C (Fig. 2).

Table 1: Chemical analyses of representative iron ore sample

Content	Wt. %
Fe(T)	63.12
Al ₂ O ₃	1.55
SiO ₂	2.57
S	0.012
P	0.043
Mn	0.217
Na ₂ O	0.090
K ₂ O	0.052
TiO ₂	0.090
LOI	9.95

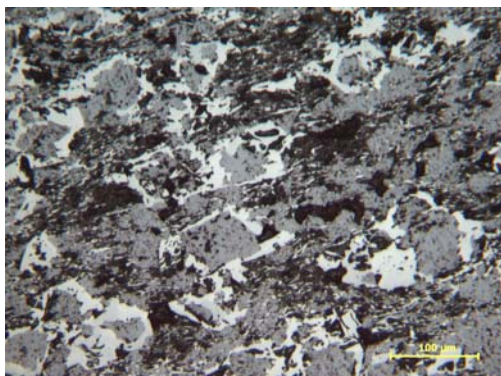


Fig. 1a: Optical micrograph of untreated (GRI-0) iron ore.

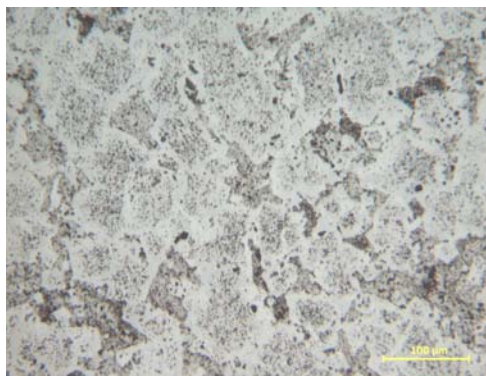


Fig. 1b: Optical micrograph of heat treated iron ore at 400°C (GRI-400).

TG-DTA of GRI-0 (Fig. 2) indicates multiple weight losses in the ranges 25–225 (~2.0%), 225–410 (~5.2%), 410–670 (~1.3%) and > 670°C (~2%) with only endothermic DTA peaks. The first stage weight loss (~5%) is attributed to physically adsorbed water molecules. The second and third stage losses mainly attributed to release of structural water from hydrous oxides. The last stage loss is mainly attributed to conversion of hematite to magnetite. The total weight loss (~10.5%) compare well with the data obtained from loss of ignition.

FT-IR spectra of untreated and heat treated iron are presented in Fig. 3. The broad absorption band in the range 3470–3480 cm^{-1} and moderately intense band at $\sim 1660 \text{ cm}^{-1}$ in all samples are attributed to O-H stretching and bending modes of vibrations.^[18] This indicates the structural water is not completely lost even 400°C. The band at 3170 cm^{-1} , attributes to bulk hydroxyl stretching, is disappeared when heated at 400°C. The O-H bending bands of Fe-OH appear at 906 and 814 cm^{-1} while Fe-O stretching band appears at 550 cm^{-1} .

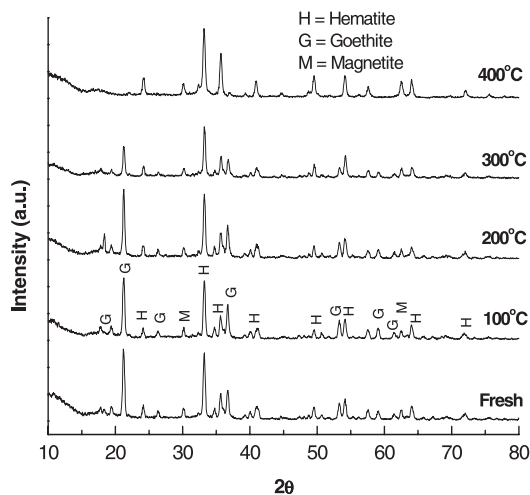


Fig. 2: X-ray powder diffraction of untreated and heat treated iron ore samples.

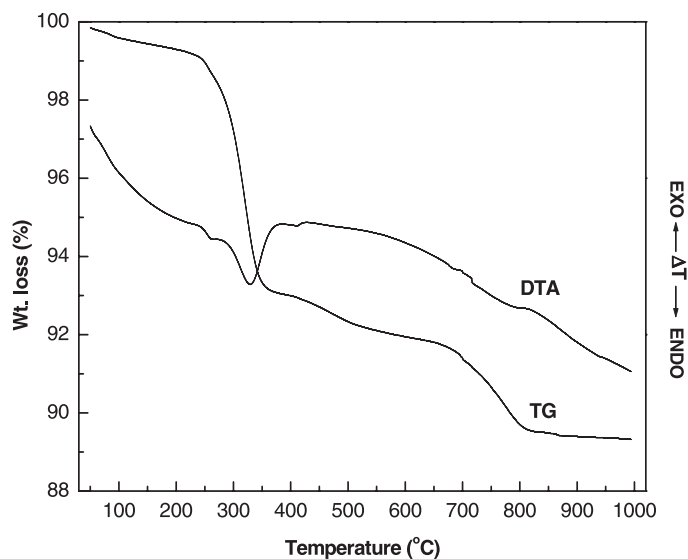


Fig. 3: TG-DTA of untreated iron ore sample (GRI-0) in air.

The point of zero charge (PZC), measured by acid-base potentiometric titration, is found to be 7.5. Keeping the complexity of materials, the value is well within the range of values reported for goethite (7.8–8.4) and hematite (5.7–8.5).

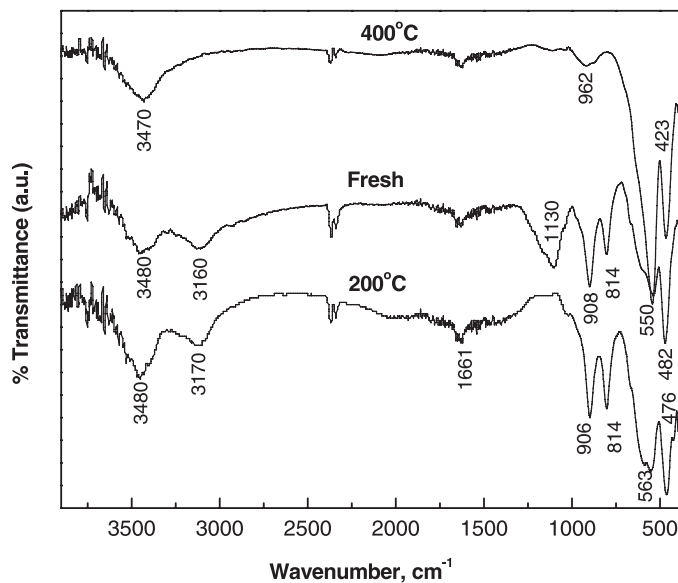


Fig. 4: FT-IR spectra of untreated and heat treated iron ore.

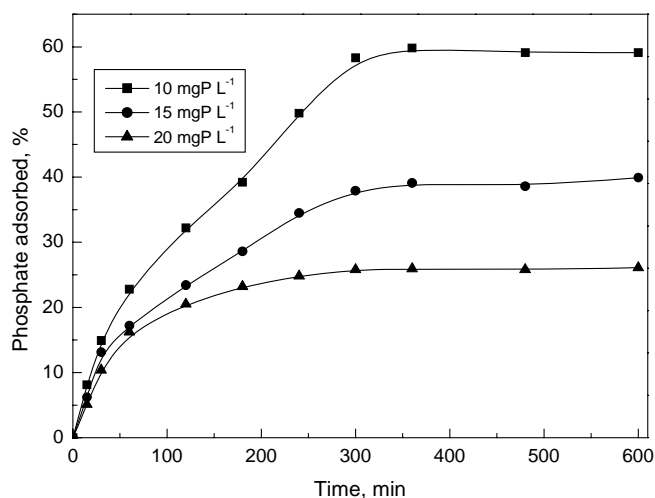


Fig. 5: Time profile of phosphate adsorption over GRI-0 (1.0 gL^{-1}) at pH ~ 5.5.

Adsorption studies

The time profiles of adsorption experiments at varying phosphate concentration indicate that about 6 h is required to attain the adsorption equilibrium (Fig. 5). Under identical set of conditions, the adsorption of phosphate practically remains same in between pH ~3–5 followed by progressive decrease in the adsorption with increase of pH up to ~11.0. Depending on the pH of the adsorbing medium, phosphate exist in different ionic forms; H_2PO_4^- is most abundant below pH 7.2 while HPO_4^{2-} is prevalent in between pH 7.2 and 12. As the pH of the adsorbing medium increases below pH_{zpc} (7.5), the surface charge of GRI-0 becomes less positive which in turn decrease the electrostatic interaction between H_2PO_4^- and GRI surface. As a result the percentage of phosphate adsorption decreases (Fig. 6). Further increase in pH above pH_{zpc} , the surface of GRI-0 becomes negatively charged which leads sharp decrease in adsorption of phosphate as HPO_4^{2-} .

It is evident from Fig. 7 that the percentage adsorption of phosphate decreases with increase of initial phosphate concentration and as expected there is an increase phosphate uptake from ~2.7 to 5.0 mgP g^{-1} of GRI-0. On the other hand, the phosphate adsorption does not increase linearly with increase of adsorbent dose from 1 to 10 g L^{-1} . The equilibrium adsorption data with varying initial phosphate concentrations are fitted to most widely used adsorption models *viz.* Freundlich and Langmuir models. The Langmuir model is better fitted yielding a maximum monolayer adsorption capacity of 5.6 mgP g^{-1} which compares well with the value of maximum phosphate uptake (~ 5.0 mgP g^{-1}). It is seen that the phosphate adsorption is strongly influenced by heat treatment of GRI-0. The phosphate uptake is increased with increasing temperature of heat treatment, attains a maximum value at ~ 300°C and then decreases progressively on further increase of temperature of heat treatment. This may be attributed to either increase of adsorption active sites in GRI due to weight loss or structural changes in GRI leading to higher surface area. The results of desorption of adsorbed phosphate on GRI-0 show that adsorbed phosphate is completely desorbed in to solution at pH ~12 (Fig. 6). This indicates that the phosphate adsorption on GRI-0 is completely reversible and the adsorbent may be reused further.

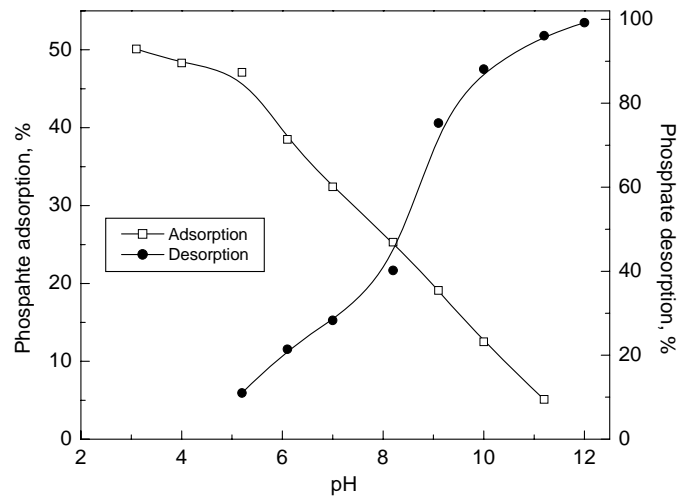


Fig. 6: Effect of pH on phosphate adsorption over untreated iron ore (GRI-0).

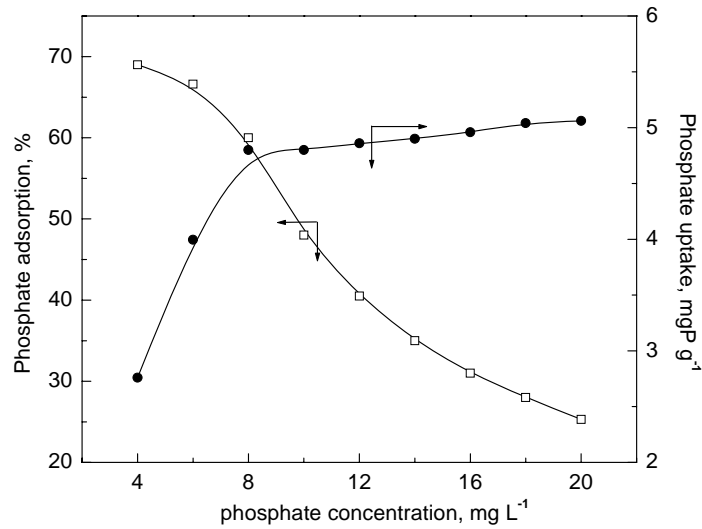


Fig. 7: Effect of concentration on phosphate adsorption over untreated iron ore (GRI-0).

CONCLUSIONS

The physicochemical characterizations of iron ore fines, collected from the open cast iron mines of Daitari, Keonjhar, show the presence of substantial amount of goethite along with hematite and magnetite as the other iron phases. On heating at 400°C, the goethite phase of untreated iron ore is completely transformed into hematite. The untreated and heat treated iron ores show potential for adsorption of phosphate from its aqueous solution. The material can be exploited further as a potential adsorbent for removal of anionic contaminants including phosphate from wastewaters.

REFERENCES

- [1] Chitrakar, R., Tezuka, S., Sonoda, A., Sakane, K., Ooi, K. and Hirotsu, T., 2006, *J. Colloid Interface Sci.*, **298**, p. 602.
- [2] Luengo, C., Brigante, M., Antelo, J. and Avena, M., 2006, *J. Colloid Interface Sci.*, **300**, p. 511.
- [3] Peleka, E.N. and Deliyanni, E.A., 2009, *Desalination*, **245**, p. 357.
- [4] Huang, X., 2004, *J. Colloid Interface Sci.*, **271**, p. 296.
- [5] Nowack, B. and Stone, A.T., 2006, *Water Res.*, **40**, p. 2201.
- [6] Rovira, M., Giménez, J., Martínez, M., Martínez-Lladó, X., Pablo, J., Martí, V. and Duro, L., 2008, *J. Hazard. Mater.*, **150**, p. 279.
- [7] Le Zeng, Xiaomei Li, Jindun Liu, 2004, *Water Res.*, **38**, p. 1318.
- [8] Spiteri, C., Cappellen, P.V. and Regnier, P., 2008, *Geochim. Cosmochim. Acta*, **72**, p. 3431.
- [9] Guo, H., Stüben, D. and Berner, Z., 2007, *Appl. Geochem.*, **22**, p. 1039.
- [10] Zhang, W., Singh, P., Paling, E. and Delides, S., 2004, *Miner. Engg.*, **17**, p. 517.
- [11] Pirillo, S., Ferreira, M.L. and Rueda, E.H., 2009, *J. Hazard. Mater.*, **168**, p. 168.
- [12] Costa, R.C.C., Moura, F.C.C., Ardisson, J.D., Fabris, J.D. and Lago, R.M., 2008, *Appl. Catal., B: Environ.*, **83**, p. 131.
- [13] Huang, H.H., Lu, M.C. and Chen, J.N., 2000, *Water Res.*, **35**, p. 2291.
- [14] Centi, G., Perathoner, S., Torre, T. and Verduna, M.G., 2000, *Catal. Today*, **55**, p. 61.
- [15] Andreozzi, R., Caprio, V. and Marotta, R., 2003, *Water Res.*, **37**, p. 3682.
- [16] Du, W., Xu, Y. and Wang, Y., 2008, *Langmuir*, **24**, p. 175.
- [17] Huang, C.P. and Ostavic, F.G., 1978, *J. Environ. Eng. Div. ASCE*, **104**, p. 863.
- [18] Nakamoto, K., 1997, *Infrared Spectra of Inorganic and Coordination Compounds, Part B*, 5th Edn., John Wiley and Sons, New York.